ORIGINAL ARTICLE

Volume 18 Issue 2 2023

DOI: 10.21315/aos2023.1802.OA01

ARTICLE INFO

Submitted: 02/01/2023
Accepted: 03/12/2023
Online: 20/12/2023

Positive Pressure and Negative Pressure Irrigation Dynamics with Different Needle Designs Using Computational Fluid Dynamics

Nur Farhana Wan[a], Nurul Ain Ramlan[a*], Nik Zarina Nik Mahmood[a], Ahmad Hussein Abdul Hamid[b]

[a]*Centre of Comprehensive Care Studies, Faculty of Dentistry, Universiti Teknologi MARA, 47000 Sungai Buloh, Selangor, Malaysia*

[b]*School of Mechanical Engineering, College of Engineering, Universiti Teknologi MARA, 40450 Shah Alam, Selangor, Malaysia*

[*]Corresponding author: ainramlan@uitm.edu.my

To cite this article: Wan NF, Ramlan NA, Mahmood NZN, Hamid AHA (2023). Positive pressure and negative pressure irrigation dynamics with different needle designs using computational fluid dynamics. *Arch Orofac Sci*, **18**(2): 125–137. https://doi.org/10.21315/aos2023.1802.OA01

To link to this article: https://doi.org/10.21315/aos2023.1802.OA01

ABSTRACT

This study aimed to investigate the irrigation dynamics of the positive pressure side-vented (SV) needle, EndoVac (micropores) needle and modified apical negative pressure (mANP) open-ended needle using computational fluid dynamics (CFD). A simulation of a prepared root canal (conical frustum) of 15 mm length with an apical diameter of 0.40 mm following Protaper F4 apical preparation was created using three-dimensional (3D) CAD software. The 3D simulated needle of SV 30G needle, EndoVac with micropores needle and mANP, 30G flat open-ended needle were also created. The irrigation dynamics were evaluated through transient CFD simulations. In addition, the irrigation dynamics of mANP at 0.2 mm, 0.5 mm, and 1.0 mm short from the working length were also assessed. The EndoVac and mANP showed negative apical static pressure and streamline patterns able to reach the apical region, thus indicating negligible extrusion. Meanwhile, SV showed positive apical static pressure and almost nonexistent streamlines beyond the needle tip. The SV showed the highest wall shear stress (WSS) magnitude of 1030Pa whereas Endovac (161 Pa) and mANP1 (258 Pa). However, SV revealed lower average WSS (10 Pa) compared to mANP1 (13 Pa) and mANP2 (11 Pa). This is due to SV developed a localised maximum WSS opposite the open vent area only therefore, uneven distribution of WSS. The EndoVac system developed a localised maximum WSS in the pair of micropores furthest away from the apical. CFD analysis of the EndoVac, mANP and SV showed different technique approach, needle design and needle depths insertion affect the irrigation dynamics pattern and magnitude.

Keywords: *Computational fluid dynamics; EndoVac; negative pressure; positive pressure; wall shear stress*

INTRODUCTION

Effective chemo-mechanical preparation plays a crucial role in achieving a favourable outcome during endodontic treatment. It involves carefully choosing suitable instruments and irrigation methods. The irrigant employed should have the ability to reach the working length while also eliminating the smear layer and

microorganisms (Miller & Baumgartner, 2010). The utilisation of a syringe and needle instrument for irrigation, employing a positive pressure irrigation system, is a widely used method. However, it is essential to exercise caution to prevent the inadvertent extrusion of the irrigant beyond the apex of the tooth (Trope, 2010). According to Perez *et al.* (2017), it was demonstrated that positioning the needle 1 mm shorter than the working length resulted in greater removal of hard-tissue debris. However, it is noteworthy that positive pressure with a side-vented needle typically delivers solutions within a range of 0 to 1.0 mm beyond the tip of the needle (Munoz & Camacho-Cuadra, 2012; Boutsioukis & van der Sluis, 2015). This revealed that positive pressure irrigation is insufficient for reaching the apical third of the root canal (Munoz & Camacho-Cuadra, 2012) due to stagnation plane (Gulabivala *et al.*, 2010). Hence, new irrigants and irrigating devices are developed to improve root canal disinfection in endodontic practice (Munoz & Camacho-Cuadra, 2012).

The EndoVac system uses a negative pressure approach in which irrigant delivered in the pulp chamber is sucked down the root canal through a unique thin needle design (Haapasalo *et al.*, 2010). Apical negative pressure has been demonstrated to be effective in addressing the challenge of effectively delivering irrigation to the most apical regions of the root canal (Hülsmann & Hahn, 2000). Additionally, it has been found to reduce the risk of irrigant extrusion (Mitchell *et al.*, 2010; Jamleh *et al.*, 2016; Konstantinidi *et al.*, 2017). Apical negative pressure appears to be capable of removing the vapor lock, resulting in increased irrigation flow and apical root canal debridement (Brunson *et al.*, 2010). Numerous studies have documented enhanced effectiveness in the removal of the smear layer at the apical region when employing negative-pressure irrigation systems (Karade *et al.*, 2017; Suman *et al.*, 2017; Widjiastuti *et al.*, 2018). Many studies on the efficacy of the EndoVac system seem to suggest that this system is the "gold standard" of apical negative pressure irrigation (Miller & Baumgartner, 2010; Jamleh *et al.*, 2016). Even though EndoVac seems to be a promising delivery system, the microcannula holes may come into contact with the root canal wall and get blocked (Abarajithan *et al.*, 2011). EndoVac was also reported to generate the lowest wall shear stress (WSS), proportional to the produced flow rate. Additionally, WSS plays a critical role in determining the mechanical impact of irrigation (Chen *et al.*, 2014; Loroño *et al.*, 2020), as it influences the removal of debris, smear layer, and biofilms from the root canal wall (Boutsioukis, Verhaagen, Versluis, Kastrinakis & van der Sluis, 2010).

In recent times, computational fluid dynamics (CFD) studies have shown considerable potential in examining the flow pattern of irrigants in the root canal system (Boutsioukis, Verhaagen, Versluis, Kastrinakis & van der Sluis, 2010; Haapasalo *et al.*, 2010). CFD analysis revealed that flow patterns of irrigants, apical pressure, velocity, and WSS differed depending on the irrigation method employed (Boutsioukis, Verhaagen, Versluis, Kastrinakis, Wesselink *et al.*, 2010; Chen *et al.*, 2014; Loroño *et al.*, 2020). It is important to note that most CFD studies analysed EndoVac with a micropore needle as the negative pressure irrigation technique. Thus, there is a need to investigate the flow pattern and magnitude of other needle designs and needle depth insertions used in negative pressure irrigation techniques using CFD. Therefore, this study aimed to investigate the irrigation dynamics of the modified apical negative pressure (mANP) with an open-ended needle in terms of WSS, streamlines, and apical pressure using computational fluid dynamics. The data are compared with the Endovac negative pressure system with micropore needle and the positive pressure system with side-vented needle under similar operating condition.

MATERIAL AND METHODS

The root canal setup was designed as a geometrical frustum of a cone, with the root canal's apical terminus designed as an impermeable wall and no simulation for the apical constriction and foramen as shown in Fig. 1 (Chen *et al.*, 2014). The length of the root canal model was set at 15 mm, with a diameter of 0.40 mm at the apical point following Protaper F4 apical preparation (6% taper) (Suman *et al.*, 2017). Instrumentation to size F4/#40 coincides with an apical diameter of 0.40 mm with a 6% taper required for efficient irrigation for both positive and negative pressure systems (Brunson *et al.*, 2010). In addition, to ensure sufficient irrigant replacement at the working length, (Boutsioukis, Verhaagen, Versluis, Kastrinakis, Wesselink *et al.*, 2010) discovered that a canal with a 6% taper is ideal for a 30G side-vented needle positioned at 1 mm from the working length.

One type of needle design for the positive pressure approach was chosen which is the side-vented needle (SV) (A 30G, Max-i-Probe needle Dentsply/Tulsa Dental, York, PA, USA) and two types of needles have been considered for the negative pressure approach, i.e. the micropore EndoVac system (Sybron Endo, Orange, CA, USA) and the 30G flat open-ended needle (a 30-G KerrHawe Irrigation Needle, KerrHawe SA, Bioggio, Switzerland) for modified apical negative pressure (mANP). The mANP used the same approach as EndoVac which is a negative pressure technique; however, instead of using a micropore needle, mANP used an open-ended needle design. To the best of the authors' knowledge, there is no study that has been conducted investigating an open-ended needle design using a negative pressure approach. Thus, there is a need to investigate the efficacy of mANP. Furthermore, a study by Boutsioukis, Verhaagen, Versluis, Kastrinakis, Wesselink *et al.* (2010), showed that different needle depth insertions using the positive pressure technique affect the WSS and apical pressure. Therefore, the present study will also investigate the irrigation dynamics of mANP at different needle depth insertions.

The root canal was first modelled in CAD software (CATIA V5, Dassault Systèmes SE, France). The needle volume is then removed from the root canal volume through Boolean subtraction, which leaves the fluid domain only. To mesh the fluid domain, a block domain consisting of 389,120 hexahedral elements is first generated. The fluid domain is then imported to the block domain in stereolithography (STL) format and meshed using snappyHexMesh, a mesh generator utility in the OpenFOAM software (*OpenCFD* Ltd, Bracknell, United Kingdom).

A grid independence study was performed by monitoring the maximum and average WSS, which has a significant impact on the effectiveness of smear layer removal. Furthermore, these parameters are known to be sensitive to the grid resolution, particularly in the near-wall region. Errors relative to the case with the highest resolution were defined as a monitor for each case. A demanding case of mANP placed 0.2 mm short of the working length was chosen for the test. The results are presented in Table 1. It shows the case with fine mesh achieved at worst a 3.79% error and is used hereafter. The mesh quality was monitored through the cells' skewness and non-orthogonality. The EndoVac and mANP fluid domains consist of 4,467,753 and 4,454,001 hexahedra cells, respectively, with respective average non-orthogonality (maximum skewness) of 5.247 (3.174) and 5.04 (3.174).

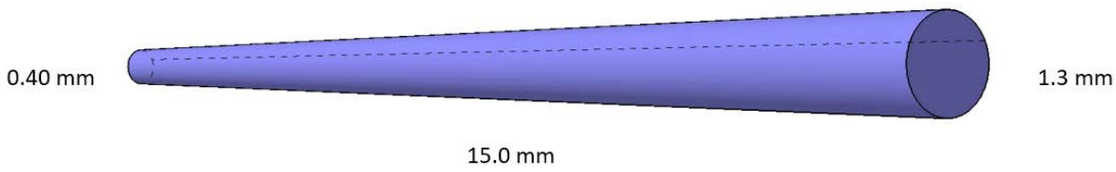

Fig. 1 A 3D root canal simulation design (Chen *et al.*, 2014).

Table 1 Percent uncertainties as a function of total cells arising from the grid independence study using mANP needle

Mesh	Number of cells	Error of maximum WSS (%)	Error of average WSS (%)
Coarse	2,967,564	3.25	7.24
Fine	4,467,753	2.32	3.79
Finest	8,477,458	–	–

The methods of irrigation were divided into three groups. Group 1 (EndoVac) consisted of a closed-ended with micropore needle by (SybronEndo, Orange, CA, USA) using the negative pressure approach; Group 2, modified apical negative pressure (mANP) with a 30G flat open-ended needle (a 30-G KerrHawe Irrigation Needle, KerrHawe SA, Bioggio, Switzerland) using negative pressure approach; and Group 3 with a 30G side-vented (SV) needle (Max-i-Probe needle, Dentsply/Tulsa Dental, York, PA, USA) using the positive pressure approach. The micropore needle of EndoVac consisted of 12 radially arranged holes, each 0.10 mm in diameter, positioned between 0.2 mm and 0.7 mm from the tip of the needle (Chen *et al.*, 2014). The micropore needle is placed at the apex following the manufacturer's protocol (Suman *et al.*, 2017). The specification for a 30-gauge cylindrical needle includes an external diameter of 0.320 mm and an internal diameter of 0.196 mm (Boutsioukis, Verhaagen, Versluis, Kastrinakis & van der Sluis, 2010). Group 2 (mANP) with an open-ended needle design was simulated at three different needle depths of insertion (0.2 mm, 0.5 mm, and 1.0 mm short from the working length) to assess the flow pattern and magnitude. The SV needle in Group 3 consisted of a side vent that was positioned on one side of the needle and modelled as a 0.5 mm slit, positioned 1.0 mm from the tip of the needle (Loroño *et al.*, 2020). The SV needle tip is placed 1.0 mm short from the working length, as this depth of insertion revealed better cleaning efficacy (Perez *et al.*, 2017).

For all groups, the inlet flow rate was set at 6 mL/min as the common velocity in clinical practice (Gao *et al.*, 2009). The positive pressure (SV), the inlet flow rate was set at 6 mL/min at the top of the needle, the flow then passed through the side vent at the same flow rate. The top of the root canal lumen was specified as an outlet flow boundary at an atmospheric pressure of 101.325 kPa (Gao *et al.*, 2009). For Group 2 (EndoVac) and Group 3 (mANP), the inlet flow rate was set at 6 mL/min at the top of the root canal lumen, and the flow was then sucked through the micropores for EndoVac and the open-ended needle for mANP.

The root canal is assumed to be filled with 3% NaOCl irrigant, which is simulated and modelled as Newtonian fluid with kinematic viscosity $\nu = 9.6555 \times 10^{-7}$ m^2s^{-1} (Liu *et al.*, 2020). The governing equations (momentum and continuity) were solved by the finite volume solver *pimpleFoam*, which uses the PIMPLE algorithm from the OpenFOAM code library (Weller *et al.*, 1998). The solver was previously validated by (Robertson *et al.*, 2015). To further validate the solver

used in the present study, flows through an orifice plate were simulated and the discharge coefficients at various Reynolds numbers were compared with data from ISO 5167-2:2003. The results are depicted in Fig. 2. It was found that, when compared to the data provided in the ISO 5167-2:2003, the present CFD simulations were found to accurately predict the discharge coefficients. At the highest Reynolds number of 50,000, the highest error of discharge coefficient was 3.7%. It is also worth noting that the trend of discharge coefficient with a variation of Reynolds number is strikingly similar.

The transient analysis is carried out using k-ω SST turbulence model, with time step sizes ranging between 3×10^{-6} s and 5×10^{-6} s. An initial time step size of $\Delta t = 10^{-4}\ L/U_{\infty}$ was imposed, and the values were automatically adjusted to match the specified maximum CFL. The turbulent intensity and the eddy viscosity ratio were set at 5% and 10%, respectively, following (Loroño *et al.*, 2020). The flow is allowed to develop until start-up transients have attenuated.

Statistical Analysis

No statistical analysis was needed as all simulations were run under the same conditions. In a simulated model, the data is generated using mathematical algorithms or rules that are programmed into the model. The model produces a set of outputs based on these algorithms, which can be analysed directly without the need for statistical analysis.

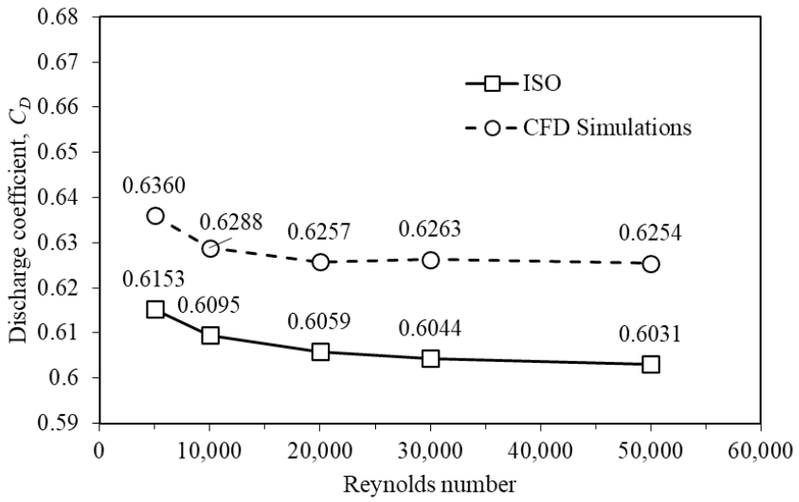

Fig. 2 Discharge coefficient plotted against Reynolds number.

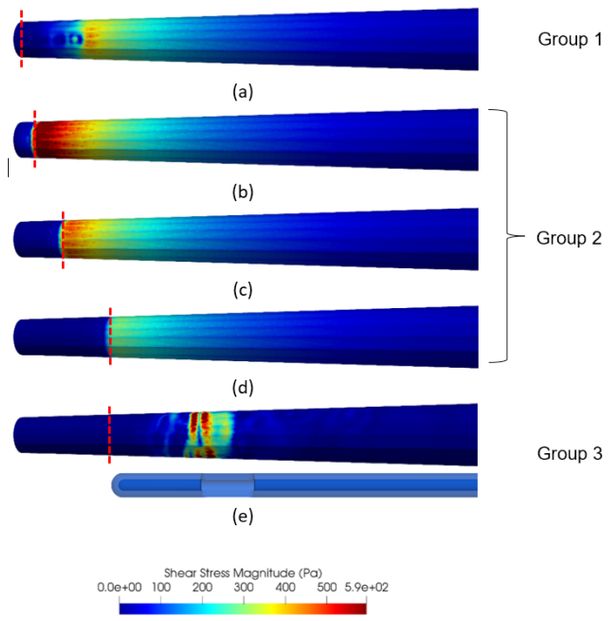

Fig. 3 Magnitude of WSS for (a) EndoVac, (b) mANP1, (c) mANP2, (d) mANP3, and (e) SV positive pressure. The red lines indicate the approximate location of the needle tip.

RESULTS

The instantaneous WSS distribution is presented in Fig. 3. The shear stress pattern on the canal wall was similar for mANP, regardless of the needle depth insertion. In general, the maximum WSS occurs close to the tip of the open-ended needles. Whereas the EndoVac shear stress pattern showed a localised maximum WSS at a distant area from the tip, even though the needle tip was placed at the apex. For the SV case, the regime of maximum WSS is localised to a small area near the tip of the vent.

Fig. 4 shows the WSS magnitude of the canal wall for different irrigation systems. SV showed the highest maximum WSS, followed by mANP1, mANP2, EndoVac, and mANP3. However, the average WSS of SV is lower than that of mANP1 and mANP2. Table 2 summarises the magnitude values of WSS, average WSS, and apical static pressure.

Fig. 5(a) reveals the EndoVac WSS pattern. The EndoVac system, however, produces a different pattern of shear stress distribution on the canal wall than the open-ended needle. The flow developed a local maximum of WSS in the vicinity of the pair of micropores furthest away from the apical. Fig. 5(b) presents the distribution of axial velocity through the micropores. It is noted that the average axial velocity is decreasing almost linearly with the distance of the micropores from the needle inlet. It is also noteworthy that the peak axial velocity occurs offset from the pore central axis, particularly for the pair of micropores furthest away from the apical.

Both the EndoVac and mANP provide good irrigant replacement as the streamlines can reach the apex, as shown in Fig. 6. However, SV shows almost no existence of irrigant replacement beyond the needle tip. According to Fig. 7, EndoVac and mANP show the z-component of irrigant velocity present up to the apical end. Whereas Fig. 8 for SV shows no existence of a z-component of irrigant velocity beyond the needle tip.

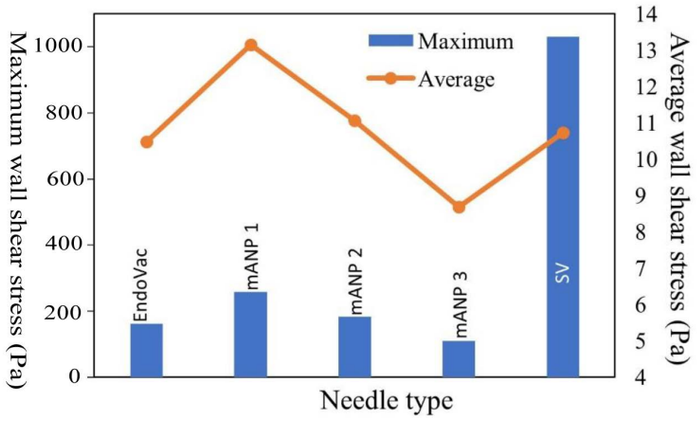

Fig. 4 WSS magnitude of the canal wall for EndoVac, mANP1, mANP2, mANP3, and SV positive pressure.

Table 2 Discharge coefficient, apical static pressure, maximum WSS, and average WSS of different irrigation systems

Needle	Discharge coefficient	Apical static pressure (kPa)	Maximum canal WSS magnitude (Pa)	Average canal WSS magnitude (Pa)
EndoVac	0.3227	−1.9742	161.24	10.48
mANP 1	0.5703	−9.8808	258.57	13.15
mANP 2	0.2651	−11.0729	183.52	11.06
mANP 3	0.1969	−14.8996	109.04	8.68
SV	0.0417	6.9051	1030.75	10.72

(a)

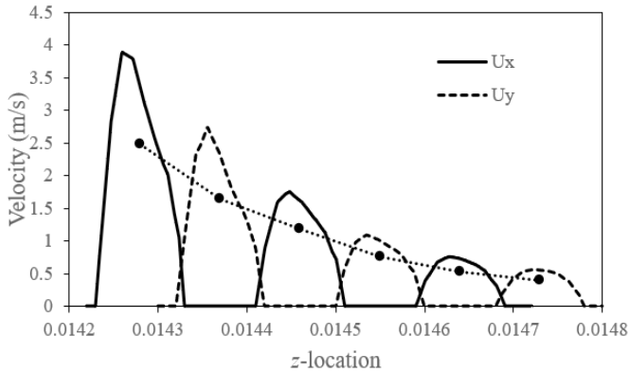

(b)

Fig. 5 (a) Contour plot of U_y velocity component on an x-normal sliced plane of an EndoVac system, and (b) the corresponding axial velocity distribution flowing through the micropores in both x- and y-normal sliced planes. The circular symbols represent the average flow velocity plotted at the corresponding centre of the pores.

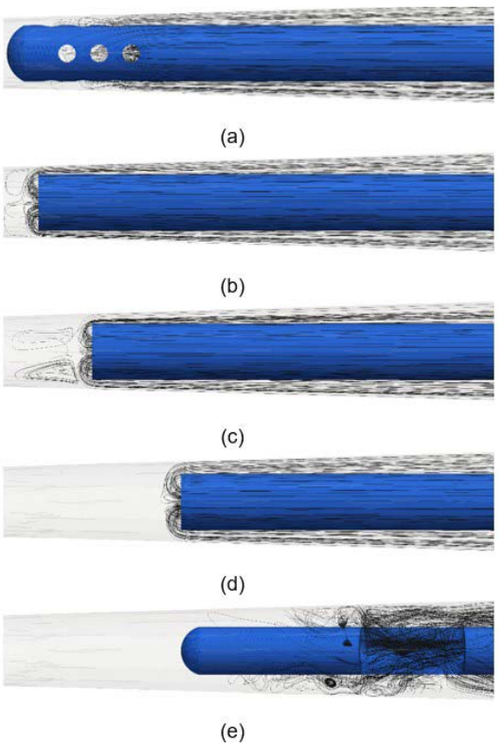

Fig. 6 Streamlines for internal flow fields for (a) EndoVac, (b) mANP1, (c) mANP2, (d) mANP3, and (e) SV positive pressure from the front plane.

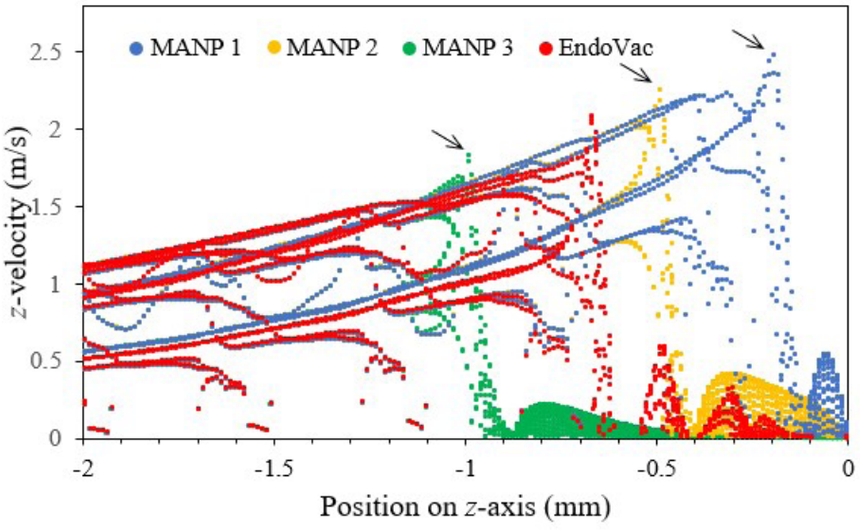

Fig. 7 Distribution of the z-component of irrigant velocity plotted against the position on the longitudinal axis of the root canal for the negative pressure approach. The arrows indicate the respective locations of the needle tips for the EndoVac and mANP.

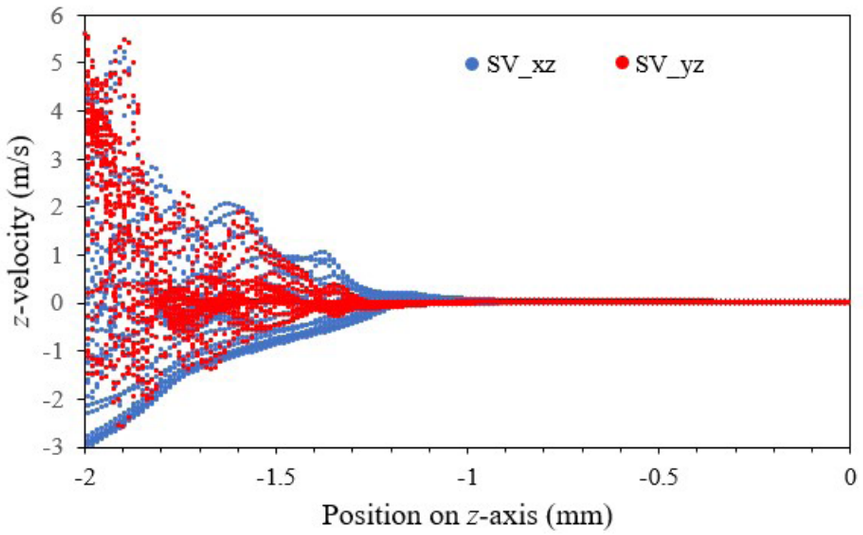

Fig. 8 Distribution of the z-component of irrigant velocity against the position on the longitudinal axis of the root canal for the SV positive pressure approach. (It is interesting to note that the irrigant replacement is almost non-existent beyond the needle tip).

DISCUSSION

Wall Shear Stress (WSS)

It is obvious from Fig. 3 and Fig. 4 that the placement of the needle is crucial in determining the efficacy of the mANP irrigation system, which can be evaluated through the distribution and magnitude of shear stress along the canal wall (Boutsioukis, Verhaagen, Versluis, Kastrinakis, Wesselink *et al.* 2010). The mANP placed 0.2 mm short of the working length resulted in a maximum WSS of approximately 41% and 136% higher than the 0.5 mm and 1 mm counterparts. This observation is attributed to the fact that the irrigant velocity near the wall is increased when the space between the needle and the root canal is reduced. Furthermore, it is observed in this case that there is a local high shear stress region on the canal wall beyond the needle tip, indicating good debridement efficacy in the region. This observation is unique and not observed in other cases. It is also noted that the maximum WSS is concentrated on a very limited area as the distance between the needle tip and root canal apex increases.

In Fig. 3, the regime of high WSS for the SV case is limited to a small area near the tip of the vent. This is in agreement with a previous study by Chen *et al.* (2014) where a high shear stress area was confined to a limited area on the canal wall directly adjacent to the side vent. In addition, (Boutsioukis & van der Sluis, 2015) showed that side-vented needle produces high maximum WSS confined near their tip, on the wall opposite the needle outlet. As expected, SV positive pressure produces the highest WSS with 1030 Pa, whereas the highest WSS in the negative pressure group is only around 258 Pa for mANP1 and 161 Pa for EndoVac. These results are similar to those of Chen *et al.* (2014) and Loroño *et al.* (2020), who revealed that EndoVac produces the lowest WSS, proportional to the flow rate produced by the apical negative pressure irrigation. Although the maximum WSS for the SV case is significantly higher than the other cases, the average value is almost similar to the mANP2 case. The open-ended needle of the positive pressure technique exhibits approximately symmetrical maximum WSS all around the needle tip (Boutsioukis & van der Sluis, 2015) and this statement is in accordance with this study, which uses a

negative pressure approach. The reduction of the area between the needle and the canal wall in mANP1 and mANP2 thus produces a more evenly distributed maximum WSS near the open-ended needle tip. Meanwhile, the SV needle shows localised max WSS opposite the open vent area only. Therefore, the uneven distribution of WSS contributes to the lower average WSS.

The EndoVac system in Fig. 5(a), however, produces a different pattern of WSS distribution on the canal wall than the open-ended needle. The flow developed a local maximum of WSS in the region of the pair of micropores furthest away from the apical. This observation is attributed to the fact that more than half (i.e. ≈ 58%) of the fluid is forced to flow through these holes, as evidenced in Fig. 5(a). The remaining 29% and 13% of the total flow seep through the second and third pair of micropores, respectively. This observation is opposite to what has been observed by Boutsioukis, Verhaagen, Versluis, Kastrinakis, Wesselink *et al.* (2010), where the most intense jet was observed to form through the pair of outlets that is closest to the apical. This is attributed to the different irrigation techniques, i.e., positive in the latter while negative in the present study. The limitation of EndoVac was that most of the irrigant was aspirated through the furthest inlet away from the tip, thus less irrigant replacement at the apical tip compared to the mANP.

Discharge Coefficient

The discharge coefficient is an important functional parameter characterising the irrigant exchange, which subsequently plays a crucial role in the debridement efficacy of an irrigation of root canals. The discharge coefficient is determined by the ratio of the actual to the ideal rate of flow. The theoretical flow rate through the injection nozzle is represented by the steady-flow orifice equation:

$$Q_{theoretical} = \mathrm{A}\sqrt{\frac{2\Delta P}{\rho}}$$

where Q is liquid volume flow rate, A is needle cross-section area, ρ is irrigant density and ΔP is pressure drop across the needle.

Table 2 summarises the rate of irrigant flow and discharge coefficient for the investigated irrigation system. A higher discharge coefficient means that the system can deliver the same amount of irrigation solution to the root canal with lower aspiration power. It was found that the discharge coefficient is highest when the mANP is placed 0.2 mm short of the working length (i.e. the mANP1 case). The reason for this observation is due to the higher velocity of the irrigant in the axial direction (z-component of velocity) and a better irrigant replacement relative to other mANP cases (see Fig. 6 and Fig. 7), which resulted in a lower static pressure in the local region and thus lower flow resistance. It is also noted that the static pressure at the apical decreased with the increase in the gap between the needle tip and the root canal apex, which is associated with a lower axial z-velocity magnitude of irrigant (Boutsioukis, Verhaagen, Versluis, Kastrinakis, Wesselink *et al.*, 2010).

Streamlines and Irrigant Replacement

In a positive pressure method, the streamlines indicate the route of fluid particles released from the needle inlet. However, in the negative pressure method, the streamlines indicate the route of fluid particles aspirated into the needle inlet. In other words, streamlines provide information on how far the irrigant can reach the apical region. Thus, they provide information about irrigant replacement (Bulgu *et al.*, 2022).

Irrigant replacement extended up to the working length for both negative pressure techniques (EndoVac and mANP system). These values are comparable to Chen *et al.* (2014) who demonstrated maximum apical penetration of the irrigant using EndoVac. Interestingly, Fig. 8 of the side vented needle showed there is almost no existence of irrigant replacement beyond the needle tip. This is in accordance with

Boutsioukis *et al*. (2009), where when irrigating at a very low flow rate (0.01 mL/s), almost no irrigant refreshment is reached apically to a closed-ended needle/SV, but an effective flow rate (0.26 mL/s) might provide refreshment up to 1 mm apically to the needle. Chen *et al*. (2014) also produced almost similar results when irrigating at 9 mL/min, which is a higher flow rate than the current study and revealed irrigant replacement extended only 0.5 mm from the needle tip. Thus, this result is comparable to Boutsioukis *et al*. (2009) statement that flow rate influences the irrigant replacement.

Apical Static Pressure

It was discussed in a previous study that high apical pressure tends to increase the potential of irrigant extrusion (Loroño *et al*., 2020; Bulgu *et al*., 2022). However, the threshold of pressure that determines the risk of extrusion remains unknown. Both mANP and EndoVac revealed negative apical static pressure, hence the negligible risk of extrusion. Interestingly, Table 2 revealed that all mANP groups showed higher negative apical pressure values compared to the EndoVac. This might be due to the open-ended needle design (mANP) that allows irrigants to be aspirated at the apical end compared to the EndoVac, which uses a close-ended needle with a micropore design. The results indicated that closed-ended needles have a lower apical pressure, whereas open-ended needles have a higher apical pressure, which is consistent with other studies (Bulgu *et al*., 2022). However, the SV needle of positive pressure produces the highest apical static pressure, around 6 Pa.

Overall, this study provides a fluid dynamics perspective of the positive pressure and negative pressure irrigation techniques with different needle designs and needle depth insertions. According to Boutsioukis, Verhaagen, Versluis, Kastrinakis, Wesselink *et al*. (2010), the tip design of the irrigation needle influences the flow pattern, flow velocity, and apical wall pressure. From the results and discussion of this study, it is acceptable to recommend using a mANP2 (0.5 mm gap) open-ended needle using a negative pressure approach clinically, as it showed comparable average WSS to SV positive pressure. In addition, with negative apical static pressure and irrigant replacement reaching the apical end, it indicates better cleaning efficacy in the apical region and reduces the risk of irrigant extrusion. However, further research is required to evaluate the relationship between the WSS magnitude and the irrigation efficacy.

CONCLUSION

The CFD analysis showed that different needle designs and needle depth insertions affect the irrigation dynamics pattern and magnitude. Both EndoVac and mANP resulted in negative apical static pressure, thus indicating a low risk of extrusion. The streamlines for both methods indicated effective irrigant replacement in the apical region, suggesting improved irrigation efficacy. Conversely, the SV needle showed positive apical static pressure and limited streamlines beyond the needle tip. In terms of WSS magnitude, the average WSS of mANP1 and mANP2 of the negative pressure approach was comparable to the SV of the positive pressure approach. Therefore, the open-ended needle design employing negative pressure (mANP) proves to be a safe and comparable alternative to the SV positive pressure approach.

REFERENCES

Abarajithan M, Dham S, Velmurugan N, Valerian-Albuquerque D, Ballal S, Senthilkumar H (2011). Comparison of Endovac irrigation system with conventional irrigation for removal of intracanal smear layer: An in vitro study. *Oral Surg Oral Med Oral Pathol Oral Radiol Endod*, **112**(3): 407–411. https://doi.org/10.1016/j.tripleo.2011.02.024

Boutsioukis C, Lambrianidis T, Kastrinakis E (2009). Irrigant flow within a prepared root canal using various flow rates: A computational fluid dynamics study. *Int Endod J*, **42**(2): 144–155. https://doi.org/10.1111/j.1365-2591.2008.01503.x

Boutsioukis C, van der Sluis LWM (2015). Syringe irrigation: Blending endodontics and fluid dynamics. In: Basrani B (ed.), *Endodontic Irrigation*. Cham: Springer, pp. 45–64. https://doi.org/10.1007/978-3-319-16456-4_3

Boutsioukis C, Verhaagen B, Versluis M, Kastrinakis E, van der Sluis LW (2010). Irrigant flow in the root canal: Experimental validation of an unsteady computational fluid dynamics model using high-speed imaging. *Int Endod J*, **43**(5): 393–403. https://doi.org/10.1111/j.1365-2591.2010.01692.x

Boutsioukis C, Verhaagen B, Versluis M, Kastrinakis E, Wesselink PR, van der Sluis LWM (2010). Evaluation of irrigant flow in the root canal using different needle types by an unsteady computational fluid dynamics model. *J Endod*, **36**(5): 875–879. https://doi.org/10.1016/j.joen.2009.12.026

Brunson M, Heilborn C, Johnson DJ, Cohenca N (2010). Effect of apical preparation size and preparation taper on irrigant volume delivered by using negative pressure irrigation system. *J Endod*, **36**(4): 721–724. https://doi.org/10.1016/j.joen.2009.11.028

Bulgu S, Yıldızeli A, Çadırcı S, Yıldırım S (2022). Computational investigation of the tip effects of various root canal needles on irrigation performance. *Essent Dent*, **1**(1): 30–37. https://doi.org/10.5152/essentdent.2021.21007

Chen JE, Nurbakhsh B, Layton G, Bussmann M, Kishen A (2014). Irrigation dynamics associated with positive pressure, apical negative pressure and passive ultrasonic irrigations: A computational fluid dynamics analysis. *Aust Endod J*, **40**(2): 54–60. https://doi.org/10.1111/aej.12027

Gao Y, Haapasalo M, Shen Y, Wu H, Li B, Ruse ND *et al.* (2009). Development and validation of a three-dimensional computational fluid dynamics model of root canal. *J Endod*, **35**(9): 1282–1287. https://doi.org/10.1016/j.joen.2009.06.018

Gulabivala K, Ng YL, Gilbertson M, Eames I (2010). The fluid mechanics of root canal irrigation. *Physiol Meas*, **31**(12): R49–R84. https://doi.org/10.1088/0967-3334/31/12/R01

Haapasalo M, Shen Y, Qian W, Gao Y (2010). Irrigation in endodontics. *Dent Clin North Am*, **54**(2): 291–312. https://doi.org/10.1016/j.cden.2009.12.001

Hülsmann M, Hahn W (2000). Complications during root canal irrigation – Literature review and case reports. *Int Endod J*, **33**(3): 186–193. https://doi.org/10.1046/j.1365-2591.2000.00303.x

Jamleh A, Fukumoto Y, Takatomo Y, Kobayashi C, Suda H, Adorno CG (2016). A comparison between two negative pressure irrigation techniques in simulated immature tooth: An ex vivo study. *Clin Oral Investig*, **20**(1): 125–131. https://doi.org/10.1007/s00784-015-1489-1

Karade P, Chopade R, Patil S, Hoshing U, Rao M, Rane N, Chopade A, Kulkarni A (2017). Efficiency of different endodontic irrigation and activation systems in removal of the smear layer: A scanning electron microscopy study. *Iran Endod J*, **12**(4): 414–418. https://doi.org/10.22037/iej.v12i4.9571

Konstantinidi E, Psimma Z, Chávez de Paz LE, Boutsioukis C (2017). Apical negative pressure irrigation versus syringe irrigation: A systematic review of cleaning and disinfection of the root canal system. *Int Endod J*, **50**(11): 1034–1054. https://doi.org/10.1111/iej.12725

Liu L, Ye W, Shen C, Yao H, Peng Q, Cui Y *et al*. (2020). Numerical investigation of irrigant flow characteristics in curved root canals with computational fluid dynamics method. *Eng Appl Comput Fluid Mech*, **14**(1): 989–1001. https://doi.org/10.1080/19942060.2020.1792349

Loroño G, Zaldivar JR, Arias A, Cisneros R, Dorado S, Jimenez-Octavio JR (2020). Positive and negative pressure irrigation in oval root canals with apical ramifications: A computational fluid dynamics evaluation in micro-CT scanned real teeth. *Int Endod J*, **53**(5): 671–679. https://doi.org/10.1111/iej.13260

Miller TA, Baumgartner JC (2010). Comparison of the antimicrobial efficacy of irrigation using the EndoVac to endodontic needle delivery. *J Endod*, **36**(3): 509–511. https://doi.org/10.1016/j.joen.2009.10.008

Mitchell RP, Yang SE, Baumgartner JC (2010). Comparison of apical extrusion of NaOCl using the EndoVac or needle irrigation of root canals. *J Endod*, **36**(2): 338–341. https://doi.org/10.1016/j.joen.2009.10.003

Munoz HR, Camacho-Cuadra K (2012). In vivo efficacy of three different endodontic irrigation systems for irrigant delivery to working length of mesial canals of mandibular molars. *J Endod*, **38**(4): 445–448. https://doi.org/10.1016/j.joen.2011.12.007

Perez R, Neves AA, Belladonna FG, Silva EJNL, Souza EM, Fidel S *et al*. (2017). Impact of needle insertion depth on the removal of hard-tissue debris. *Int Endod J*, **50**(6): 560–568. https://doi.org/10.1111/iej.12648

Robertson E, Choudhury V, Bhushan S, Walters DK (2015). Validation of OpenFOAM numerical methods and turbulence models for incompressible bluff body flows. *Comput Fluids*, **123**: 122–145. https://doi.org/10.1016/j.compfluid.2015.09.010

Suman S, Verma P, Prakash-Tikku A, Bains R, Kumar-Shakya V (2017). A comparative evaluation of smear layer removal using apical negative pressure (EndoVac), sonic irrigation (EndoActivator) and Er: YAG laser -An in vitro SEM study. *J Clin Exp Dent*, **9**(8): e981–e987. https://doi.org/10.4317/jced.53881

Trope M (2010). Treatment of the immature tooth with a non-vital pulp and apical periodontitis. *Dent Clin North Am*, **54**(2): 313–324. https://doi.org/10.1016/j.cden.2009.12.006

Weller HG, Tabor G, Jasak H, Fureby C (1998). A tensorial approach to computational continuum mechanics using object-oriented techniques. *Comput Phys*, **12**(6): 620–631. https://doi.org/10.1063/1.168744

Widjiastuti I, Rudyanto D, Yuanita T, Bramantoro T, Widodo WA (2018). Cleaning efficacy of root canal irrigation with positive and negative pressure system. *Iran Endod J*, **13**(3): 398–402. https://doi.org/10.22037/iej.v13i3.20875